EQUIVALENT CIRCUITS OF MICROSTRIP DISCONTINUITIES INCLUDING RADIATION EFFECTS

A. Skrivervik, J.R. Mosig

Ecole Polytechnique Fédérale
Lausanne, Switzerland

Abstract

An efficient theoretical method for the full-wave analysis of microstrip circuit elements has been developed, taking into account effects due to surface waves and radiation. A new de-embedding process allows the derivation of equivalent circuits independent of the feed model used. Results for bends and slots are in good agreement with measurements and reduce to quasistatic predictions in the low frequency range.

INTRODUCTION

Microstrip structures and related microwave integrated circuits are now being used in frequency bands where their transverse dimensions and substrate thicknesses are no longer much smaller than the wavelength. Therefore, the development of accurate models for microstrip discontinuities, taking into account effects like dispersion and coupling due to radiation and surface waves, is an essential priority. Equivalent circuits of microstrip discontinuities (steps, bends, etc..) based on a quasistatic approach do not suffice in these cases and "full-wave" models are often required to include effects which cannot be predicted in the framework of a TEM-approximation.
Previously published works (1,2) have dealt with full-wave treatments of microstrip discontinuities like open-ends and gaps, where the surface electric current can be approximated by a longitudinal component only. Recently, Jackson (3) has generalized this approach to geometries whose description requires two components of the current, each depending on the two transverse coordinates.
From a theoretical point of view, the technique presented here can be shown to be basically equivalent to that developed in (3). However, the full-wave analysis is cast into the form of a MPIE (Mixed Potential Integral Equation) solved in space domain . The pertinent Green's functions are thus given by Sommerfeld integrals which are precomputed and tabulated. This allows a division of the microstrip structure into unequal size cells and therefore yields a great flexibility in defining geometries without unduly increasing the computational effort.
A de-embedding technique avoids the use of special basis and test functions for the excitation lines. The length of the lines to be included in the numerical procedure is relatively small compared to the wavelength, keeping the total number of unknowns to a reasonable value. In addition, there is no limitation on the number of ports.

THEORY

The mixed potential integral equation to be solved has been presented in a previous work (4). Here, we will stress only on the fact that two-dimensional rooftop basis functions and a Galerkin testing procedure are used. The final MoM matrix equation can be written as

$$\sum_j Z_{ij} I_j = V_i \quad \text{with}$$

$$Z_{ij} = j\omega \int_{Si} ds\, \mathbf{T}_i(\rho) \int_{Sj} ds'\, \overline{\overline{G}}_a(\rho|\rho') \cdot \mathbf{T}_j(\rho') +$$

$$\frac{1}{j\omega} \int_{Si} ds\, \Pi_i(\rho) \int_{Sj} ds'\, G_v(\rho|\rho')\, \Pi_j(\rho') +$$

$$Z_s \int_{Si} ds\; \mathbf{T}_i(\rho) \cdot \mathbf{T}_j(\rho)$$

where Z_S is a surface impedance (ohms/square) accounting for ohmic losses, $\overline{\overline{G}}_a$ and G_v are the pertinent space-domain Green's functions to be pre-computed with a very efficient integration routine, $\mathbf{T}_j(\rho)$ is a two dimensional vector-rooftop function and $\Pi_j(\rho)$ the corresponding 2-D pulse charge. The double surface integral is reduced to a single surface integral by a convenient change of variables. Thus the computation of every matrix term requires the evaluation of only one surface integral over a bounded domain.
Theoretically, the computed impedance or scattering port-matrix of the analyzed element is independent of the chosen feed model owing to the de-embedding process described later on. This allows the use of very simple theoretical excitations as the idealized coaxial probe (4).
This choice yields the following excitation terms:

$$V_i = \frac{1}{j\omega} \int_{Si} ds\, \Pi_i(\rho) \int_{Se} ds'\, G_v^*(\rho|\rho')\, P_e(\rho')$$

CH2725-0/89/0000-1147$01.00 © 1989 IEEE

where G_v^* is the scalar potential Green's function corresponding to a vertical dipole and P_e a single pulse function corresponding to the excitation cell S_e. Once the unknowns I_j have been computed, the derivation of the impedance port matrix proceeds along the lines described in (4).

In the theoretical analysis, the structure to be analyzed is connected to the sources through microstrip line sections (fig. 1a). A de-embedding process extracts the scattering matrix of the unknown structure (for instance the 4-port 1, 2, 3, 4 of fig. 1a) from the computed scattering matrix, which is related to planes 1', 2', 3', 4' (fig.1a).
The main advantage of this de-embedding process is to yield equivalent circuits having well defined reference planes and being independent of the excitation, which is always difficult to model. To obtain the impedance matrix of the circuit element to be analyzed, a generalized chain matrix method is used. The method is briefly illustrated here for the 4-ports of fig. 1a, and can be easily generalized to n-ports.
The analyzed structure is shown in fig.1a and its equivalent circuit is given in fig.2. The impedance matrix Z_{tot} between the reference planes 1', 2', 3', 4' is known and we wish to determine the matrix Z between the planes 1, 2, 3, 4. Prior to this, we need to obtain the 2-port matrices Z^k, k=1, 2, 3, 4. This is done by computing the chain matrix T'^k of a line of double length $l = 2\,l^k$ (fig. 1b). The chain matrix T^k of half the structure is given by $T'^k = T^k\,T^k$. Knowing T^k, we can write :

$$[u'] = [Z^{tot}][i'] \qquad [u] = [Z][i]$$

But

$$\begin{bmatrix} u'^k \\ i'^k \end{bmatrix} = [T^k] \begin{bmatrix} u^k \\ i^k \end{bmatrix} \qquad k = 1, 2, 3, 4$$

where

$$[T^k] = \begin{bmatrix} t_{11}^k & t_{12}^k \\ t_{21}^k & t_{22}^k \end{bmatrix}$$

so finally we can write :

$$[Z] = \left\{ [\mathrm{Diag}\, t_{11}] - [Z^{tot}][\mathrm{Diag}\, t_{21}] \right\}^{-1} \times \left\{ [Z^{tot}][\mathrm{Diag}\, t_{22}] - [\mathrm{Diag}\, t_{12}] \right\}$$

where

$$[\mathrm{Diag}\, t_{ij}] = \begin{bmatrix} t_{ij}^1 & 0 & 0 & 0 \\ 0 & t_{ij}^2 & 0 & 0 \\ 0 & 0 & t_{ij}^3 & 0 \\ 0 & 0 & 0 & t_{ij}^4 \end{bmatrix} \qquad i,j = 1,2$$

Once the matrix [Z] is known, the scattering matrix [S] of the structure follows by standard circuit analysis.

RESULTS

As a preliminary test, we have analyzed a section of uniform microstrip line whose characteristic impedance Z_c, predicted with standard quasi-TEM formulas, was 50 Ohms. Fig.3 shows the series impedance $Z_s = z_{11} - z_{12}$ of the T-equivalent circuit obtained with our full-wave analysis. A nonzero real part due to radiation losses is predicted, increasing in the low frequency range as the square of the frequency. As expected, the imaginary part behaves almost linearly with frequency. From its value and from similar results obtained for the parallel admittance, it is possible to recover the characteristic impedance and propagation constant whose low frequency limiting values match very well the quasi-TEM predictions. This is an useful check for the numerical accuracy of the proposed technique.
Next, we have studied a 50-ohm bend. In fig.4 we have plotted the transverse dependence of the longitudinal component of the surface current at three different distances from the discontinuity. Far away from the bend (C), we are close to an uniform line distribution. When the bend is approached (B,A), the overall longitudinal current diminishes (being transformed into a transverse component) and exhibits an asymmetrical shape, concentrating in the line's inner edge.This clearly shows the need for including both components of the current into the analysis.
Figs 5 and 6 show some interesting results concerning power conservation and reflection properties for several methods of bend compensation. While the original bend radiates 9% of the incoming power at 10 GHz ($P = |s_{11}|^2 + |s_{12}|^2 = 0.91$), we have for a mitered bend at the same frequency P>0.99 (fig.5). The mitered bend also gives the best results concerning the reflection with a SWR below 1.10 while the original bend gives an SWR of 1.50 at 10 GHz (fig.6). The round corner turns out to be the worst compensation and cutting a square gives intermediate quality results. This classification has been confirmed empirically (5).
Finally, we have analyzed a double impedance step obtained by cutting a lateral slot in the line. Figs 7 and 8 show the comparison between analysis and measurement of the equivalent T circuit of this discontinuity. Measurements have been done using a ring resonator method (5). The resonant frequencies have been measured on a HP 8510B network analyzer. This kind of indirect determination of the equivalent circuit being very sensitive, several measurements have been made to obtain average values. Theoretical values for the series impedance (parallel susceptance) agree well with measurements and predict essentially imaginary values behaving like ωL_s (ωC_p) with L_s (C_p) being almost independent of the frequency. No attempt has been made to measure the very small real parts predicted by the theory.
All these simulations and measurements have been done for a substrate where $\varepsilon_r = 2.33$, $h = 0.51$ mm and for line impedances of 50 ohms (line widths of 1.53 mm).

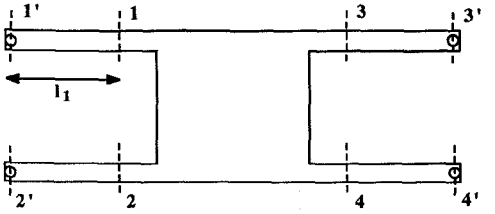

fig. 1a

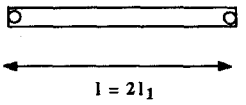

fig. 1b

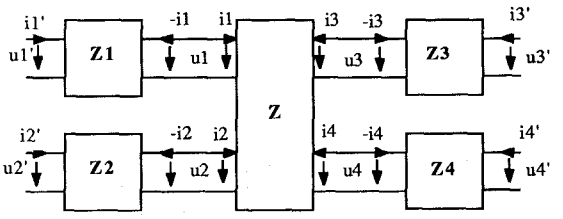

fig. 2

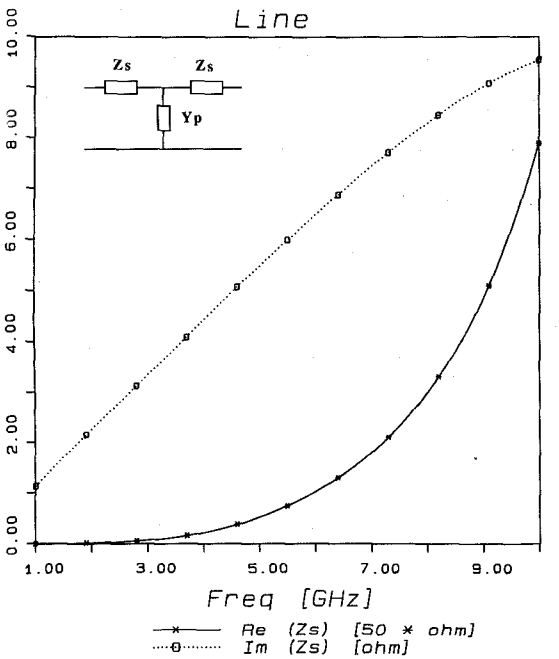

fig. 3

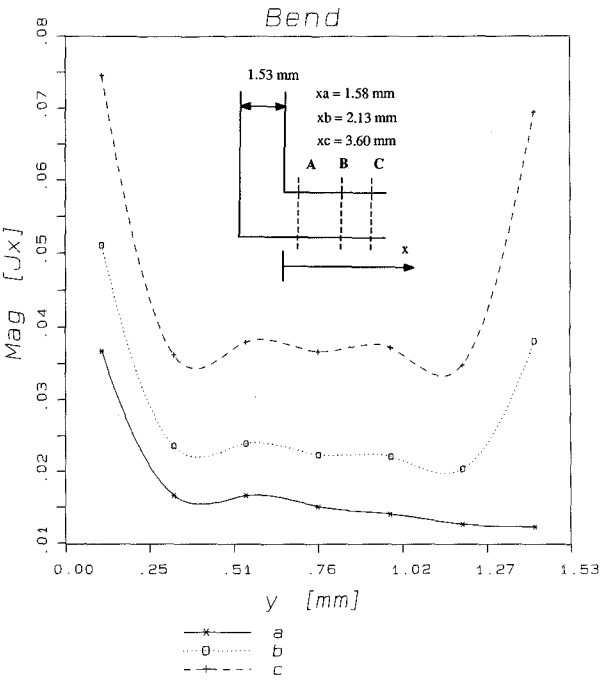

fig. 4

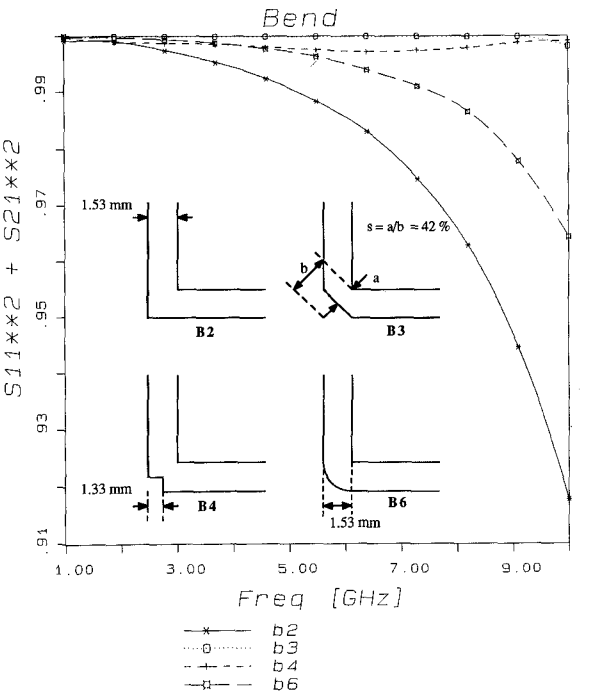

fig. 5

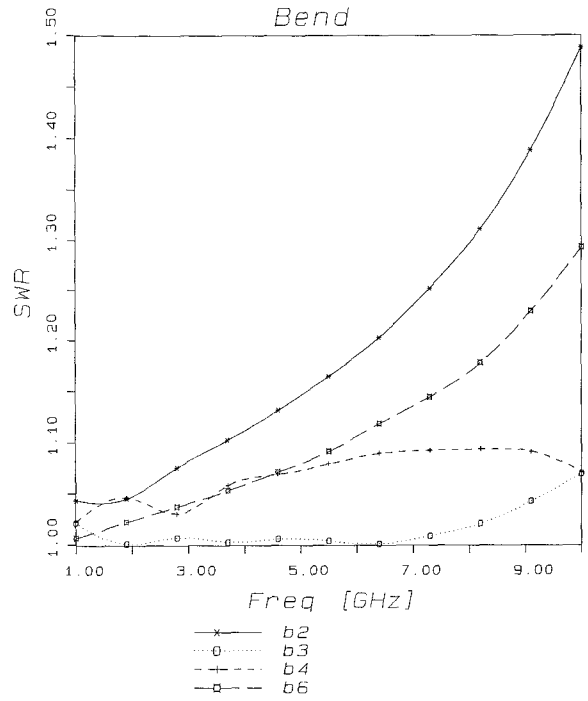

fig. 6

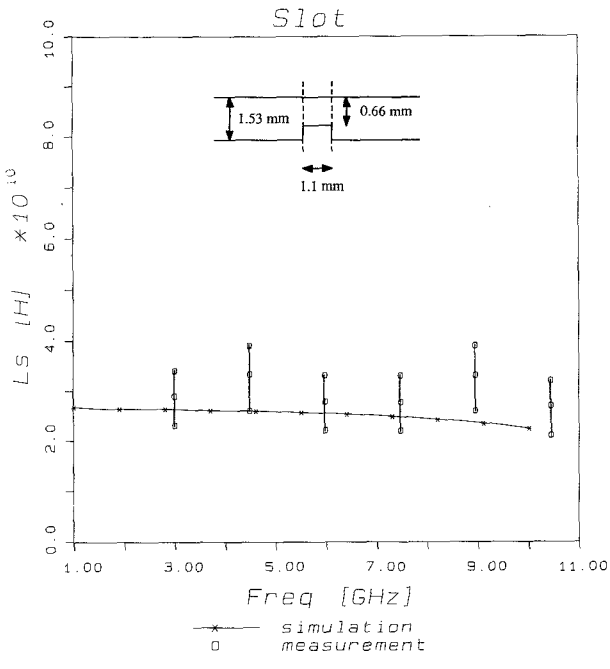

fig. 7

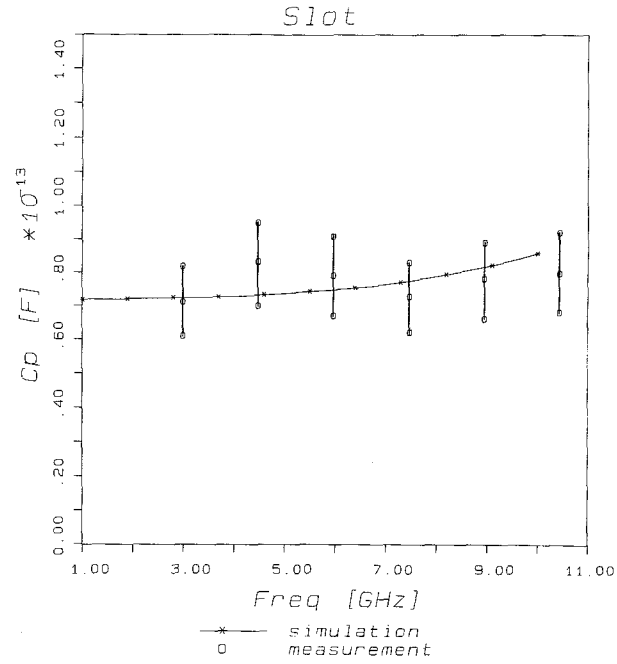

fig. 8

CONCLUSION

An efficient theoretical method for the full-wave analysis of microstrip circuit elements has been developed, taking into account effects like dispersion, coupling between elements, surface waves, ohmic and dielectric losses and radiation. A de-embedding process allows the derivation of equivalent circuits independent of the feed model used. Results are in good agreement with other theories and with measurements. The method was first tested by analyzing a segment of a uniform microstrip line, and then it was applied to several two-port discontinuities (bends, slots,...).As shown in the theory, the method is easily extendable to any N-port structure. Discontinuities on other related substrate configurations (strip-line, suspended and multilayered microstrip) could be easily analyzed with this technique by using the pertinent Green's functions.

REFERENCES

(1) R.W. Jackson and D.M. Pozar, "Full-wave analysis of microstrip open-end and gap discontinuities", IEEE Trans. on MTT., **vol. 33**, Oct. 1985, pp.1036-1042

(2) P.B. Katehi and N.G. Alexopoulos, "Frequency-dependent characteristics of microstrip discontinuities in millimeter-wave integrated circuits", IEEE Trans. on MTT., **vol. 33**, Oct. 1985, pp.1029-1035

(3) R.W. Jackson, "Full-wave, finite element analysis of irregular microstrip discontinuities", IEEE Trans. on MTT., **vol. 37**, Jan. 1989, pp.81-89

(4) J.R. Mosig, "Arbitrarily shaped microstrip structures and their analysis with a mixed potential integral equation", IEEE Trans. on MTT., **vol. 36**, Feb. 1988, pp.314-323

(5) R.K. Hoffmann, "Handbook of microwave integrated circuits", Artech House, Dedham, MA, 1988